JOURNAL OF CATALYSIS **169,** 22–32 (1997)
ARTICLE NO. CA971693

A Two-Step Transformation of the Magnesium Salt of Phosphomolybdic Acid $HMgPMo_{12}O_{40}$ Supported on Silica

J-M. Tatibouët,*,†,[1] C. Montalescot,* K. Brückman,‡ J. Haber,‡ and M. Che†

*Laboratoire de Catalyse en Chimie Organique, UMR CNRS 6503, Ecole Supérieure d'Ingénieurs de Poitiers, Université de Poitiers, 40 avenue du Recteur Pineau, 86022 Poitiers cedex, France; †Laboratoire de Réactivité de Surface, URA CNRS 1106, Université P. et M. Curie, 4 place Jussieu, 75252 Paris cedex 05, France; and ‡Institute of Catalysis and Surface Chemistry, Polish Academy of Sciences, ul. Niejapominacek, 30239-Krakow, Poland

Received October 21, 1996; revised March 12, 1997; accepted March 14, 1997

The thermal decomposition of silica-supported phosphomolybdic acid ($H_3PMo_{12}O_{40}$) has been followed by different techniques (TGA-DTA, FT-IR, and Raman spectroscopies, XRD) and methanol oxidation as a probe reaction. When Mg cations are present on the silica surface, the magnesium salt $HMgPMo_{12}O_{40}$ with Keggin structure is formed in situ on the silica surface during catalyst preparation by impregnation. The presence of Mg induces a two-step thermal decomposition of the Keggin ion by stabilizing an intermediate surface species identified to a planar oxide cluster with the same nuclearity and composition as those of the Keggin precursor. High temperature ($\geq 500^\circ$C) calcination leads to the formation of crystallized α-MoO_3. In absence of Mg, the decomposition occurs in only one step and leads to the formation of α- and β-MoO_3 in a ratio depending on the calcination temperature.

A. INTRODUCTION

Heteropolycompounds (HPC) and particularly those with the Keggin structure (Fig. 1) have been widely studied in catalysis (1–3). These compounds are very attractive models of oxide-supported catalysts since they can be regarded either as oxide clusters with controlled nuclearity and composition or as precursors of a supported oxide phase obtained after thermal decomposition of the HPC. In the latter case, the knowledge of the transformation mechanism of the HPC into oxide is paramount to control the nature of the active oxide phase obtained after thermal decomposition of supported heteropolycompounds species. One of the most important questions is to know whether the resulting oxide phase is formed of clusters with the same nuclearity and composition as those of the HPC precursor (4) or formed by surface oxides resulting from the agregation of oxides species originating from the HPC precursor. In this point of view, we can expect that a well-dispersed precursor species will lead to a well-dispersed oxide phase after thermal decomposition of the HPC. The dispersion of surface adsorbed species should roughly depend on two types of attractive interactions:

—interaction between species themselves;
—interaction between support surface and species.

If the former interaction is the most important, as in the case of water on a nonwetting surface, agregates will be obtained, whereas if the latter is predominant (water on a wetting surface), a monolayer-like deposit with high dispersion will be obtained.

A possible way to obtain a high dispersion of heteropolyacid precursor as $H_3PMo_{12}O_{40}$ could be to create, on the acid silica surface, basic sites able to form strong interactions between them and the acid precursor. Magnesium was chosen to play the role of basic center since it is strongly basic (5–8) and does not form easily a silicate compound. Moreover, in various reaction, alkaline-earth have been found to have a beneficial effect on selectivity (9, 10).

In order to investigate the decomposition mechanism of supported HPC, we have used different techniques including Raman and IR spectroscopies, X ray diffraction (XRD), thermal analysis (TGA-DTA), and the catalytic oxidation of methanol as a probe reaction able to characterize both HPC and oxide species resulting from HPC transformation, to follow the thermal transformation of silica-supported $HMgPMo_{12}O_{40}$.

B. EXPERIMENTAL

(a) Catalyst precursor preparation. Silica (XOA 400 from Rhône-Poulenc; BET surface area $\approx 376\ m^2 \cdot g^{-1}$) has been used as a support. $H_3PMo_{12}O_{40}$ (from Aldrich, A. C. S. reagent grade), referred to as HPMo was used without further purification. The water content, measured from TGA experiment, was 28.5 water molecules per Keggin unit (Fig. 2). $HMgPMo_{12}O_{40}$, referred to as MgPMo, was prepared from stoichiometric quantities of magnesium carbonate and phosphomolybdic acid in aqueous media,

[1] Corresponding author.

0021-9517/97 $25.00

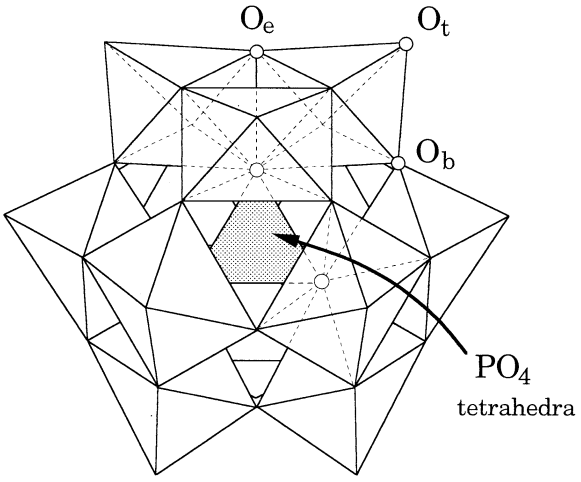

FIG. 1. Structure of the Keggin ion.

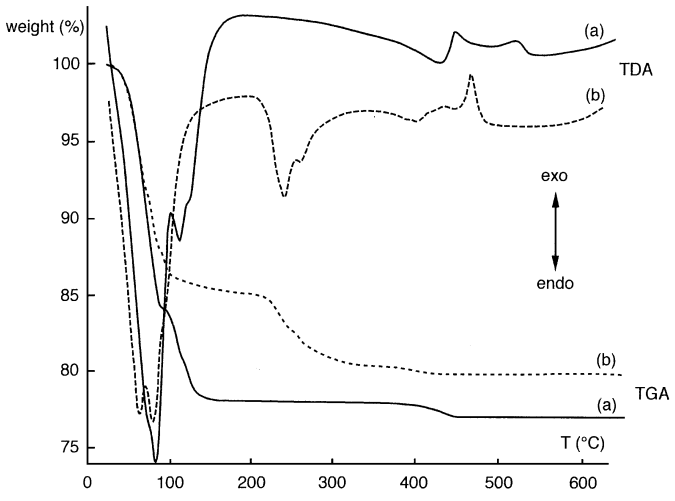

FIG. 2. TGA-DTA experiments of unsupported HPMo (a) and MgPMo (b).

according to the method described by Tsigdinos (11). The water content was determined as 26.0 water molecules per Keggin unit by TGA experiment (Fig. 2). Three series of supported catalysts were prepared by using different procedures (Table 1). The samples referred to as $MgPMo/SiO_2$ were prepared by wet impregnation of silica by an aqueous solution of MgPMo and dried overnight at 120°C. The samples referred to as HPMo/xMg–SiO_2 ($x = 1, 2$) were pepared by a two-step procedure (12) which consists to deposit Mg cations on the silica surface before the impregnation of HPMo aqueous solution in order to realize in situ, on the silica surface, the magnesium salt MgPMo (12). The first step was to deposit magnesium cations on the silica surface by wet impregnation of an aqueous solution of magnesium nitrate, followed by drying overnight at 120°C and calcination in air for 2 h at 500°C. The second step was the impregnation of the modified silica (Mg–SiO_2) by an aqueous solution of phosphomolybdic acid (HPMo) followed by drying overnight at 120°C. The amounts of Mg and HPMo were adjusted in order to ensure a Mg to HPMo molecular ratio (Mg/KU) of 1 or 2. Assuming that one Keggin unit occupies 144 $Å^2$, catalysts corresponding formally to 0.2, 0.5, and 1 monolayer (mnl) coverage were prepared for each series. As previously shown (12), we expect to realize in situ, during the impregnation procedure of HPMo, the Mg salt of HPMo, directly on the silica surface.

A Mg-free catalyst with a 0.5 monolayer coverage (0.5 mnl) was prepared for the sake of comparison, by the same procedure as for the $MgPMo/SiO_2$ sample, but starting from HPMo instead of MgPMo. This sample will be referred to as $HPMo/SiO_2$.

TABLE 1

Catalyst Preparation

Sample name	*1st step* impregnation of the SiO_2 support by: (dried at 120°C and calcined at 500°C)[a]	*2nd step* impregnation of the support by: (dried at 120°C)[a]	Coverage (mnl)	Mo (wt%)
$HPMo/SiO_2$	Pure water	Aq. solution of $H_3PMo_{12}O_{40}$	0.5	17.8
$MgPMo/SiO_2$	Pure water	Aq. solution of $HMgPMo_{12}O_{40}$	0.2	8.6
			0.5	17.8
			1.0	27.7
HPMo/1Mg–SiO_2	Aq. solution of $Mg(NO_3)_2$	Aq. solution of $H_3PMo_{12}O_{40}$	0.2	8.6
			0.5	17.8
			1.0	27.7
HPMo/2Mg–SiO_2	Aq. solution of $Mg(NO_3)_2$	Aq. solution of $H_3PMo_{12}O_{40}$	0.5	17.8

[a] After impregnation.

(b) Thermal analysis. Thermal analysis experiments were performed on a combined thermobalance-differential analysis apparatus (TGA-DTA), in order to record simultaneously the sample weight and the temperature difference between the sample and a reference located near the sample. TG Instruments STD 540 and Seiko TGA-DTA 320 were used for the thermal analysis of unsupported HPC (HPMo and MgPMo) and supported HPC, respectively. The experiments were performed under air, between room temperature and 600°C with a heating rate of 10°C/min. Sample weights were approximately 25 mg and 10 mg for supported and unsupported HPC, respectively.

(c) Infrared spectroscopy. IR spectra were recorded in KBr disks at room temperature on a FT-IR Nicolet 750 spectrophotometer with a resolution of 4 cm^{-1}, each spectrum corresponding to the sum of 32 scans.

(d) Raman spectroscopy. Raman spectra were recorded at room temperature on a Nicolet 800 FT-Raman spectrophotometer, using an Ar laser at a power as low as possible in order to avoid HPC decomposition under laser beam.

(e) X-ray diffraction (XRD) measurements. XRD patterns were recorded at room temperature on a Siemens D 500, X-ray diffractometer, using the Cu Kα radiation. XRD patterns of unsupported HPMo and MgPMo samples and of supported HPMo/SiO_2 and HPMo/xMg–SiO_2 samples at 0.5 monolayer coverage, were recorded directly after catalyst preparation (fresh samples) or after a 2 h calcination at different temperatures ranging from 300 to 500°C.

(f) Catalytic measurements. Methanol oxidation was used as a test reaction in a continuous-flow, isothermal (250°C) fixed-bed reactor (13) operating at atmospheric pressure. The composition of the reactant feed CH_3OH/O_2/He was in the molar ratio 7.1/15.5/77.4, which corresponds to a methanol partial pressure of 54 Torr. The reactant mixture was obtained by flowing an O_2/He mixture through a methanol saturator maintained at 10°C. The overall flow rate and catalyst weight were adjusted in order to secure a moderate methanol conversion not exceeding 20%. Catalytic measurements were performed at steady state, usually about 30 min after the reactant feed was contacted with the catalyst. On-line gas chromatographic analysis was used to determine the feed composition before and after passing through the catalyst. The reaction rates are expressed relatively to the methanol consumption and to the molybdenum weight.

C. RESULTS AND INTERPRETATION

The experimental results obtained with unsupported (HPMo and MgPMo) and silica-supported (HPMo/SiO_2, MgPMo/SiO_2, and HPMo/xMg–SiO_2) samples are presented below in terms of thermal stability and structural transformations of Keggin unit ($PMo_{12}O_{40}$) in various environments (silica-supported or unsupported and in the presence or absence of Mg cations).

(1) Unsupported Samples

(a) Thermal analysis. The DTA and TGA curves of unsupported starting materials (MgPMo and HPMo) are presented in Fig. 2. The DTA curve of unsupported HPMo shows two groups of endotherms at low temperature (80 and 108°C) which correspond to the loss of about 28.5 water molecules per Keggin anion, as determined from TGA curve. At higher temperatures, we observe a broad endotherm followed by a sharp exotherm centered at 439°C. These two peaks are associated with the loss of about 1.5 water molecules. A weak and broad exotherm is also visible at 508°C. The low temperature endotherms (80 and 108°C) are generally associated with the loss of crystallization water (14, 15). At higher temperature (≈400°C), the formation of water from acidic protons and oxygen belonging to the Keggin units has been proposed (14). This water, called constitution water corresponds, as expected, to ≈1.5 water molecule per Keggin unit. At the end of this weight loss, the exotherms at 439 and 508°C are assigned to the collapse of the Keggin structure and to the crystallization of the resulting oxides.

DTA of a MgPMo sample behaves quite differently, since two groups of endotherms separated by more than 100°C are visible (Fig. 2). The first one, centered at ≈80°C corresponds to the loss of 20 water molecules and the second at ≈240°C to 6 water molecules per Keggin unit. These endotherms could be assigned to the loss of crystallization water. In the high temperature region, an endotherm can be observed at 400°C, followed by two exotherms at 427 and 461°C. The endotherm at 400°C is associated with a weight loss corresponding to ≈0.5 water molecule per Keggin unit as expected for the water formation from the remaining proton (loss of constitution water).

(b) X-ray diffraction (XRD). The XRD patterns of unsupported HPMo after different calcination temperatures are presented in Fig. 3. After calcination at 400°C which corresponds to the loss of the constitution water, we observe a deep change in the XRD pattern, with the disappearance of almost all the diffraction lines observed in the noncalcined HPMo. Only unassigned broad and weak lines are still visible. By contrast, crystallized β-MoO_3 (16–20) is clearly visible after calcination at 450°C, with a small amount of α-MoO_3 (19). We can then assign the first exotherm of the TDA curve (centered at 439°C) to the β-MoO_3 crystallization. After calcination at 500°C, which corresponds to the beginning of the second exotherm (Fig. 2), only α-MoO_3 is visible on the XRD pattern, allowing to unambiguously assign the latter exotherm to the $\beta \rightarrow \alpha$-MoO_3 transformation, as expected from literature data (16, 17).

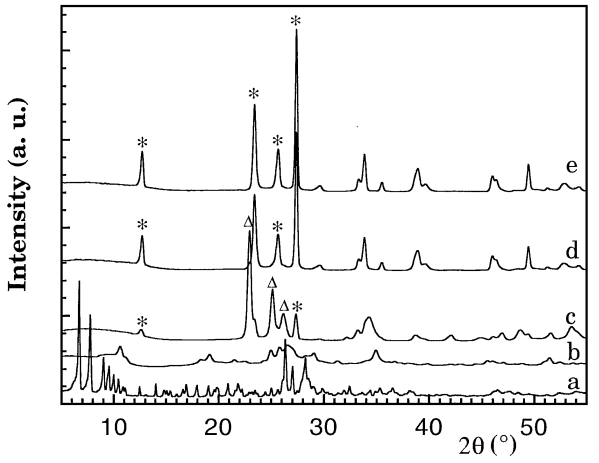

FIG. 3. XRD patterns of unsupported HPMo calcined at different temperatures: (a) uncalcined; (b) 400°C; (c) 450°C; (d) 500°C; (e) 550°C; ∗, α-MoO_3; △, β-MoO_3.

The XRD patterns of MgPMo samples calcined at various temperatures (Fig. 4) confirm the different behaviour of this sample. Up to 400°C, only broad and weak diffraction lines are visible. After calcination at 450°C, a pattern assigned to α-MoO_3 (19) is present in addition to some minor lines which could be due to a distorded form of β-MoO_3 (21). After calcination at 500°C, only α-MoO_3 is visible. From this study, it appears that the presence of Mg seems to increase the stability of the intermediate species between the hydrated Keggin ion and crystallized MoO_3 oxide (α or β). The absence of the transitory formation of the metastable β-MoO_3 phase could result to the increase of the thermal stability of this intermediate species, its transformation to crystallized oxide occuring then at a higher temperature of the upper limit of the stability domain of β-MoO_3, allowing then the only formation of α-MoO_3.

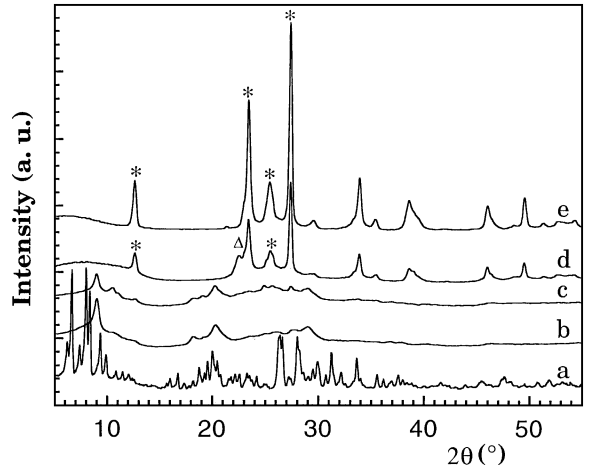

FIG. 4. XRD patterns of unsupported MgPMo calcined at different temperatures: (a) uncalcined; (b) 350°C; (c) 400°C; (d) 450°C; (e) 500°C; ∗, α-MoO_3; △, β-MoO_3.

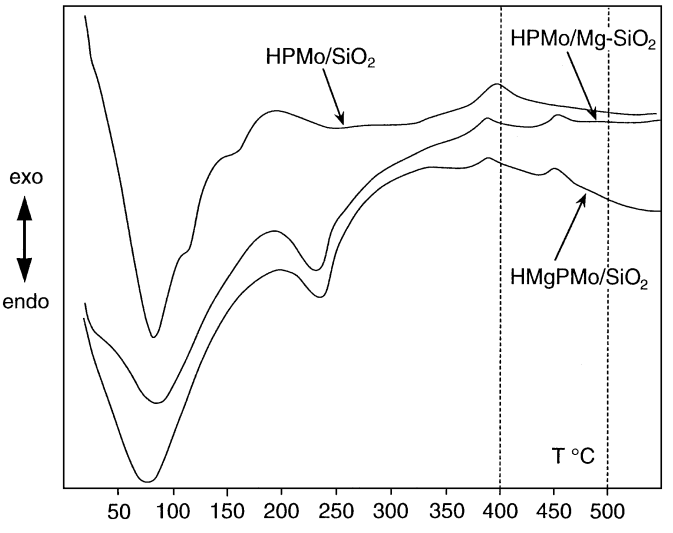

FIG. 5. DTA experiments of supported Mg-containing (HPMo/1Mg–SiO_2 and MgPMo/SiO_2) and Mg-free samples (HPMo/SiO_2); coverage = 0.5 monolayer.

(2) Supported Samples

(a) Thermal analysis. The TDA curves (Fig. 5) of Mg-containing silica-supported samples (MgPMo/SiO_2 and HPMo/1Mg–SiO_2) are quite similar, suggesting that the surface species are the same for these two samples, whatever the preparation method (12). The first endotherm (≈80°C) could be due to the sum of the thermal effects of the water desorption from silica surface and the loss of the first part of crystallization water as for unsupported MgPMo sample, whereas the second endotherm (235°C) seems only due to the loss of the second part of crystallization water, since the latter peak decreases with HPC content (Fig. 6). In the high temperature region, only two exotherms are visible

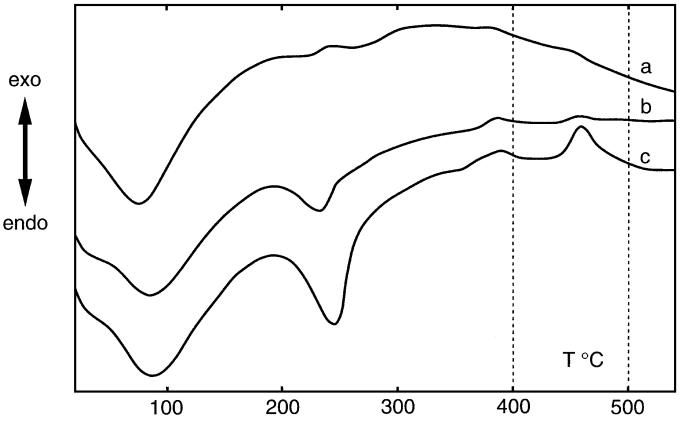

FIG. 6. DTA experiments of HPMo/1Mg–SiO_2 samples at different coverages: (a) 0.2 monolayer; (b) 0.5 monolayer; (c) 1.0 monolayer.

(385 and 452°C), but at a different temperature from that observed for the unsupported sample.

The supported HPMo/SiO_2 sample presents some differences with the supported Mg-containing samples (Fig. 5). The second endotherm at ≈240°C is very weak and broad and only one exotherm is visible in the high temperature region (395°C).

If the first exotherm at 395°C is assigned to the collapse of the Keggin structure, these results show that the $PMo_{12}O_{40}^{-3}$ anion is thermally less stable when it is supported on silica, as already observed for $SiMo_{12}O_{40}^{-4}$ (22).

It appears from these experiments that the thermal behavior of supported samples containing Mg is completely different from the corresponding unsupported HPC. In particular, the two well-defined and largely separated exotherms in the high temperature region suggest a change in the nature of surface species corresponding to each of these peaks. In order to determine the nature of the modification of these species in function of the temperature, we have characterized by various techniques (IR, Raman, XRD, and catalytic reaction) the supported samples after calcination at different temperatures (400°C and 500°C) chosen after the two exotherms at 385 and 452°C (Fig. 5).

Before their characterizations by the different techniques, the treatments were performed in the TGA-DTA apparatus, both temperature and DTA signal being simultaneously monitored.

(b) FT-IR spectroscopy. The infrared spectra of HPMo/1Mg–SiO_2 (0.5 mnl) are shown in Fig. 7. The spectrum of the fresh sample exhibits in addition to the silica bands (1100 and 800 cm^{-1}), the main bands of the Keggin units (23) at 1065 cm^{-1} (ν_{as} P–O), 978 cm^{-1} (visible as a shoulder) and 962 cm^{-1} (ν_{as} Mo=O_t), and 876 cm^{-1} (ν_{as} Mo–O_b–Mo). After calcination at 400°C, the two bands at 978 and 962 cm^{-1} are still visible with, however, a lower intensity than in the fresh sample, whereas the bands at 1065 and 876 cm^{-1} have almost completely disappeared. After high temperature treatment (500°C), only the silica bands remain clearly visible. HPMo/2Mg–SiO_2 (0.5 mnl) sample behaves similarly.

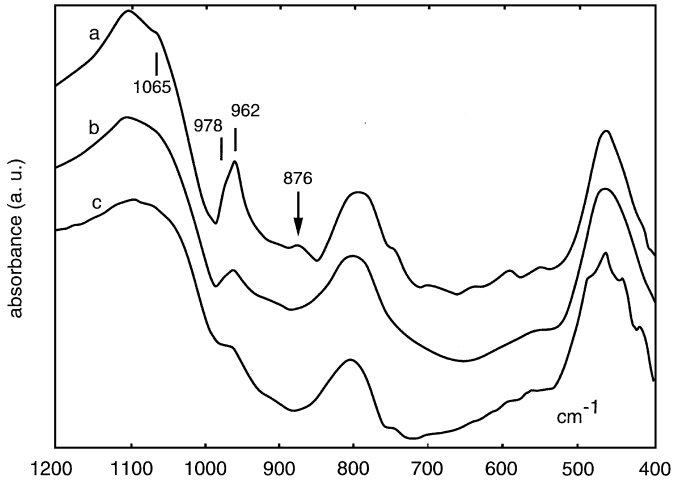

FIG. 7. FT-IR spectra of HPMo/1Mg–SiO_2 (0.5 monolayer) calcined at different temperatures: (a) fresh sample (uncalcined); (b) calcined at 400°C; (c) calcined at 500°C.

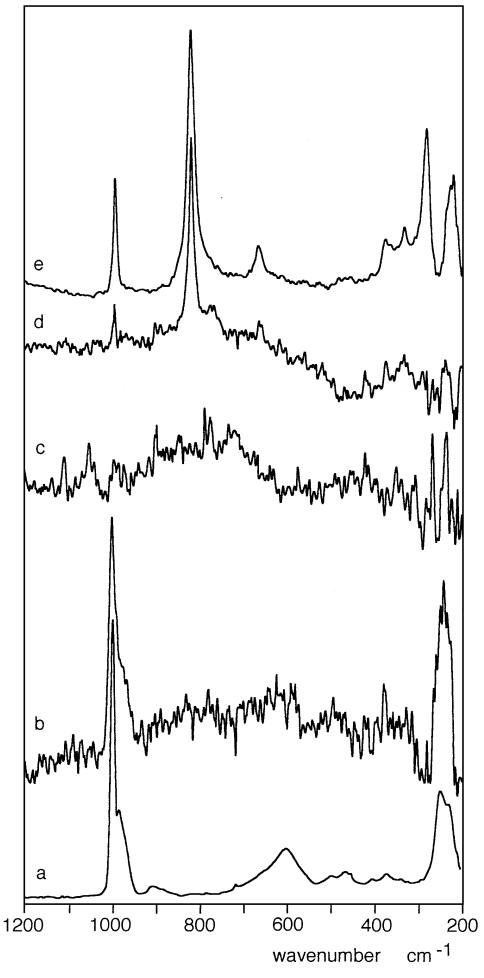

FIG. 8. Raman spectra of HPMo/1Mg–SiO_2 (0.5 monolayer) calcined at different temperatures and of unsupported MgPMo and α-MoO_3: (a) unsupported MgPMo; (b) HPMo/1Mg–SiO_2 fresh sample; (c) HPMo/1Mg–SiO_2 calcined at 400°C; (d) HPMo/1Mg–SiO_2 calcined at 500°C; (e) unsupported α-MoO_3.

(c) Raman spectroscopy. The Raman spectra of HPMo/1Mg–SiO_2 (0.5 mnl) are shown in Fig. 8. The spectrum of the uncalcined sample presents the main Raman bands of the Keggin unit (23) at 995 cm^{-1} (ν_s Mo=O_t), 981 cm^{-1} (ν_{as} Mo=O_t), and 248 cm^{-1} (ν_{as} Mo–O_p). After calcination at 400°C, no Raman signal is visible, even after accumulation of 1000 scans. After high temperature calcination, a Raman signal assigned to MoO_3 is present at 992, 820, and 666 cm^{-1}.

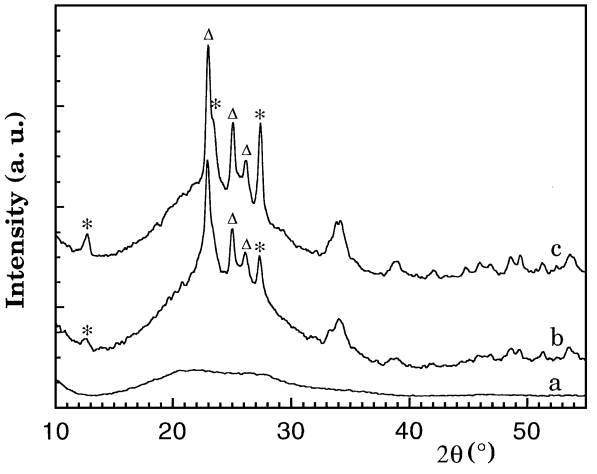

FIG. 9. XRD patterns of $HPMo/SiO_2$ (0.5 monolayer) calcined at different temperatures: (a) uncalcined; (b) 400°C; (c) 500°C; ∗, α-MoO_3; △, β-MoO_3.

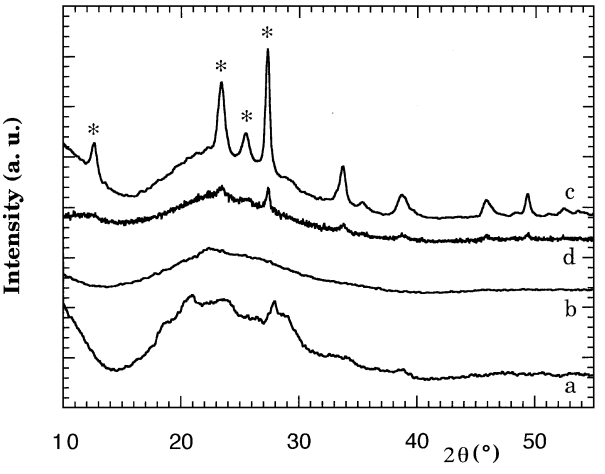

FIG. 10. XRD patterns of $HPMo/xMg–SiO_2$ (0.5 monolayer) calcined at different temperatures: $HPMo/1Mg–SiO_2$: (a) uncalcined; (b) 400°C; (c) 500°C; $HPMo/2Mg–SiO_2$: (d) 500°C; ∗, α-MoO_3.

(d) X-ray diffraction (XRD). The XRD patterns of $HPMo/SiO_2$ and $HPMo/xMg–SiO_2$ samples with a 0.5 monolayer coverage are presented in Figs. 9 and 10, respectively. The patterns are quite similar for the fresh samples, with only broad signals assigned to the silica support. After calcination at 400°C, several lines assigned to a mixture of α- and β-MoO_3 are visible for the Mg-free sample (17–19, 24, 25), whereas the XRD pattern of the Mg-containing samples does not exhibit any diffraction line.

After calcination at 500°C, the α- and β-MoO_3 lines are always visible on the Mg-free sample with, however, a better resolution, indicating an increase in the oxide cluster size. On the Mg-containing samples, only the α-MoO_3 pattern is clearly visible after calcination at 500°C on $HPMo/1Mg–SiO_2$, whereas on $HPMo/2Mg–SiO_2$ only broad and low intensities lines assignable to α-MoO_3 are visible. This behavior shows that the Keggin decomposition occurs at higher temperature when Mg cations are present and that the mechanism of Keggin ions transformation into the corresponding oxides is modified by the presence of the Mg cations.

(e) Catalytic methanol oxidation. The catalytic results are presented in Table 2 and in Figs. 11 and 12 for the samples corresponding to a 0.5 monolayer coverage on the

TABLE 2

Catalytic Behavior of Silica-Supported Samples for Methanol Oxidation (Coverage = 0.5 mnl) T_R = 250°C; $CH_3OH/O_2/He$ = 7.1/15.5/77.4 (mol%)

	$HSiMo/SiO_2$[a] Mg/KU = 0			$HPMo/SiO_2$ Mg/KU = 0			$MgPMo/SiO_2$ Mg/KU = 1			$HPMo/Mg–SiO_2$ Mg/KU = 1			$HPMo/2Mg–SiO_2$ Mg/KU = 2		
	Fresh	Calc. 400°C	Calc. 450°C	Fresh	Calc. 400°C	Calc. 500°C	Fresh	Calc. 400°C	Calc. 500°C	Fresh	Calc. 400°C	Calc. 500°C	Fresh	Calc. 400°C	Calc. 500°C
S DME (%)	66	2	2	73	19	21	37	11	10	52	10	3	24	19	18
S DHG (%)	24	64	64	17	56	59	47	67	62	35	65	60	52	68	68
S F (%)	18	35	37	13	40	44	36	49	43	25	48	40	35	58	58
S MF (%)	4	49	47	7	18	24	17	25	21	19	26	21	24	17	11
S ML (%)	12	12	11	1	21	9	9	14	25	2	11	28	15	7	12
S CO_x (%)	0	2	3	6	2	2	1	1	1	3	5	8	2	1	1
A Σ (mmol/h/gMo)	1004	80	60	1211	166	170	295	183	69	290	124	70	260	216	203
A DME	663	2	2	888	31	35	110	20	7	150	12	2	63	40	36
A DHG	241	51	39	202	93	101	139	122	42	103	80	42	136	148	137
A F	181	28	22	160	66	75	106	90	29	74	60	28	92	125	118

Note. S X = selectivity; A X = formation rate; A Σ = overall reaction rate. F = CH_2O; MF = $HCOOCH_3$; ML = $(CH_3O)_2CH_2$; CO_x = CO, CO_2; DME = CH_3OCH_3. DHG = F + 1/2MF + 1/3ML.

[a] From Ref. (22).

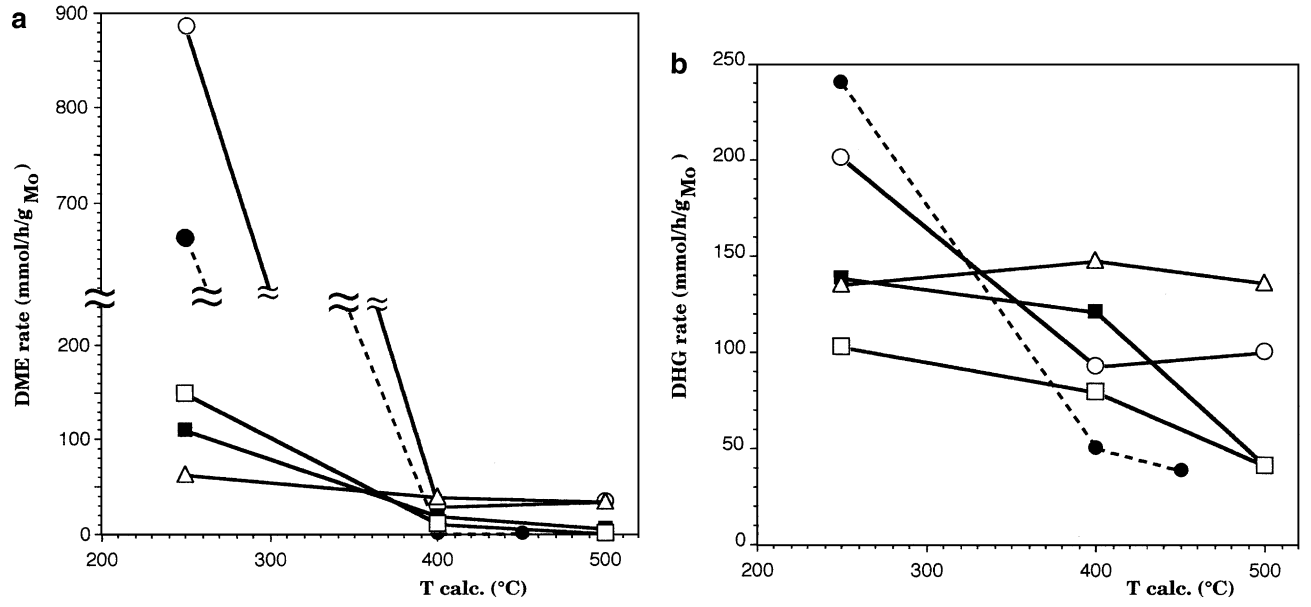

FIG. 11. Supported samples (0.5 monolayer); reaction temperature 250°C; $CH_3OH/O_2/He = 7.1/15.5/77.4$ mol%. (a) Variation of the DME (CH_3OCH_3) formation rates in function of the calcination temperature. (b) Variation of the DHG rates in function of the calcination temperature. $HSiMo/SiO_2$ (from Ref. (22)), –●–; $HPMo/SiO_2$, —○—; $MgPMo/SiO_2$, —■—; $HPMo/1Mg–SiO_2$,—□—; $HPMo/2Mg–SiO_2$, —△—.

silica support. Results from Ref. (22) are also presented, together with the results of this work, since they were obtained in similar conditions with the same kind of catalysts ($H_4SiMo_{12}O_{40}$ on silica XOA 400). We have expressed the overall redox behavior by the methanol oxidative dehydrogenation rate (DHG) which represents formally the first step of methanol oxidation if we assume that a common intermediate species (I) leads to the formation of the mild oxidation products (formaldehyde, F; methyl formate, MF; methylal, ML) as described by the following scheme:

$$CH_3OH \longrightarrow (I) \longrightarrow CH_2O \quad (F)$$
$$(I) \xrightarrow{+CH_3OH} HCOOCH_3 \quad (MF)$$
$$(I) \xrightarrow{+2CH_3OH} CH_3OCH_2OCH_3 \quad (ML)$$

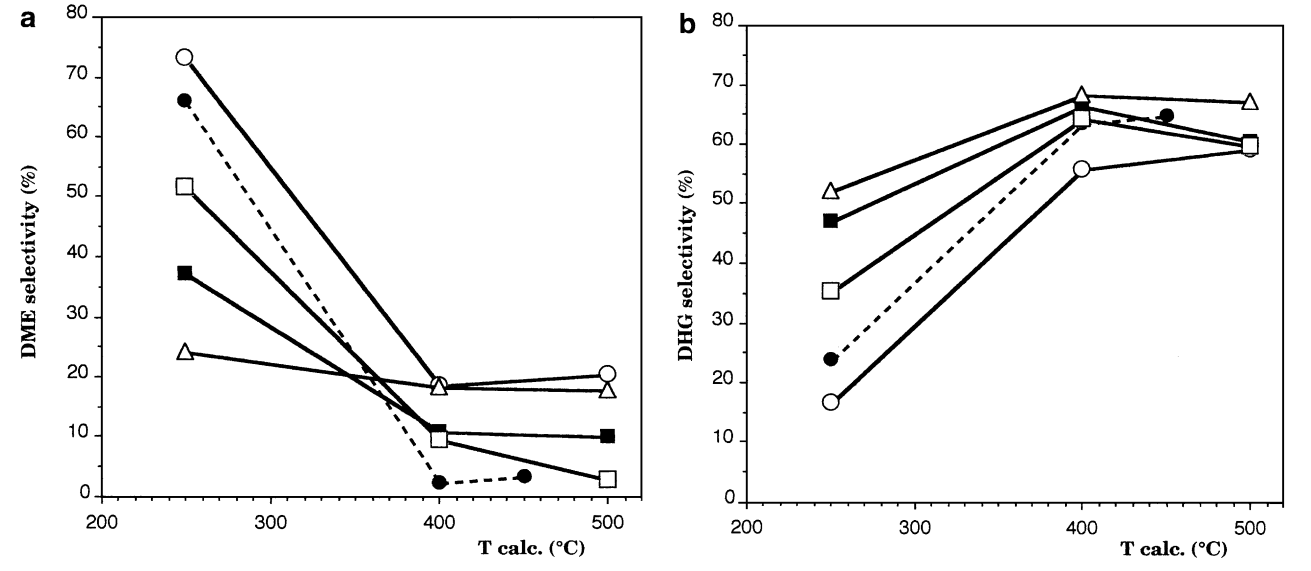

FIG. 12. Supported samples (0.5 monolayer); reaction temperature 250°C; $CH_3OH/O_2/He = 7.1/15.5/77.4$ mol%. (a) Variation of the DME (CH_3OCH_3) selectivities in function of the calcination temperature. (b) Variation of the DHG selectivities in function of the calcination temperature. Same symbols as in Fig. 11.

The DHG rate is then calculated by: DHG = F + 1/2MF + 1/3ML.

For the fresh samples, a very different catalytic behavior is observed between Mg-free and Mg-containing samples. Mg-free samples are characterized by a much higher overall reaction rate and dimethyl ether (DME) selectivity than the Mg-containing samples. The catalytic behavior observed on Mg-containing samples is consistent with the presence of $HMgPMo_{12}O_{40}$ species on the silica surface, whatever the preparation method (12). The dimethyl ether being formed on acid sites (13), the lower formation rate observed on Mg-containing samples can be explained by a lower amount of available acidic protons (27) due to the Mg salt formation. The decrease of DME formation rate and the constancy of the DHG rate when the molar ratio between Mg and Keggin unit (Mg/KU) increases from 1 to 2 confirm this interpretation.

The effect of different calcination temperatures on the catalytic behavior has been investigated on the samples corresponding to a 0.5 monolayer coverage on the silica support.

After calcination at 400°C, a dramatic decrease of the overall reaction rate is observed for Mg-free samples. This effect is also observed, but to a lower extent on Mg-containing samples. For Mg-free samples both DME and DHG rates decrease; the decrease of the DME formation rate being more pronounced than the DHG one.

For Mg-containing samples, the catalytic behavior is quite different since, even if a decrease in the DME formation rate is also observed, the DHG rate remains almost constant.

The DHG selectivity which increases for all the samples after calcination at 400°C, is always higher for the Mg-containing samples than for the Mg-free ones.

The catalytic behavior observed on Mg-containing samples could be assigned to the disappearance of the protonic acidity of the Keggin species, without significant change in the redox properties, while on the Mg-free samples it can be expected a deep transformation of the surface precursor.

The high temperature thermal treatment (450°C for $HSiMo/SiO_2$ (22), 500°C for the other samples) does not further modify significantly the catalytic behavior of the Mg-free samples. For the Mg-containing samples, the catalytic behavior seems to depend on the Mg/KU molar ratio. For Mg/KU = 1 samples, both DME formation rate and DHG rate decrease, whereas for Mg/KU = 2 sample, the catalytic behavior and the products formation rates remain unaffected.

In terms of selectivities (Fig. 12 and Table 2), the Mg-containing samples present a maximum for both formaldehyde and DHG selectivities after calcination at 400°C. This behavior is not observed for $HPMo/SiO_2$ sample where only methylal selectivity passes through a maximum, whereas formaldehyde and DHG selectivities grow with calcination temperature.

D. DISCUSSION

(1) Calcination Effect

Important structural changes of the surface species of $HPMo/1Mg–SiO_2$ samples has been shown by the two spectroscopic techniques used (FT-IR and Raman) after calcination at 400°C and 500°C. Both IR and Raman spectroscopies show that the Keggin structure is preserved in the fresh catalyst. After calcination at 400°C, the disappearance of Raman signals and the dramatic decrease of the IR band at 876 cm^{-1} indicate that the Keggin units are partly collapsed but do not yet transform into the corresponding crystallized oxides. Raman spectroscopy being very sensitive to long-distance order, the absence of signal suggests that the oxidized phase resulting from Keggin unit transformation is disordered. The almost total disappearance of the 876 cm^{-1} IR band assigned to the vibration (ν Mo–O_b–Mo) of the oxygen bonding two groups of three Mo edge-connected octahedra (Fig. 1) suggests that the Keggin units are opened after calcination at 400°C. Nevertheless, the preservation of the two bands at 978 (shoulder) and 962 cm^{-1}, characteristics of the vibration mode of the Mo=O_t bond could indicate that the Keggin units have not completely collapsed, with some parts of the Keggin structure being preserved.

After high temperature calcination, the disappearance of all the Keggin bands on the IR and Raman spectra and the presence on the Raman spectrum of characteristic features of α-MoO_3, shows unambiguously that α-MoO_3 is present on the silica surface and means that, at this temperature, the HPC to oxide transformation is completed.

From thermal analysis, Raman spectra, and XRD patterns, the first exotherm observed on the TDA curve of the $HPMo/1Mg–SiO_2$ sample cannot be assigned to β-MoO_3 formation as for unsupported HPMo. The presence of only α-MoO_3 after calcination at 500°C on the $HPMo/xMg–SiO_2$ samples, whereas on $HPMo/SiO_2$ the oxide β-MoO_3 is the main phase, suggests that a disordered species, but obviously thermodynamically favored, different from β-MoO_3 is formed after calcination at 400°C of the $HPMo/xMg–SiO_2$ samples. This species is further transformed into α-MoO_3 by calcination at 500°C (second exotherm centered at 452°C), without transitory formation of β-MoO_3, the transition temperature being too high to observe this metastable phase.

From DTA experiments which show two exotherms in the 350–500°C range for the Mg-containing samples, we can propose that the Keggin transformation into oxide upon thermal treatment occurs in two separate steps in Mg-containing catalysts ($HPMo/xMg–SiO_2$ and $MgPMo/SiO_2$).

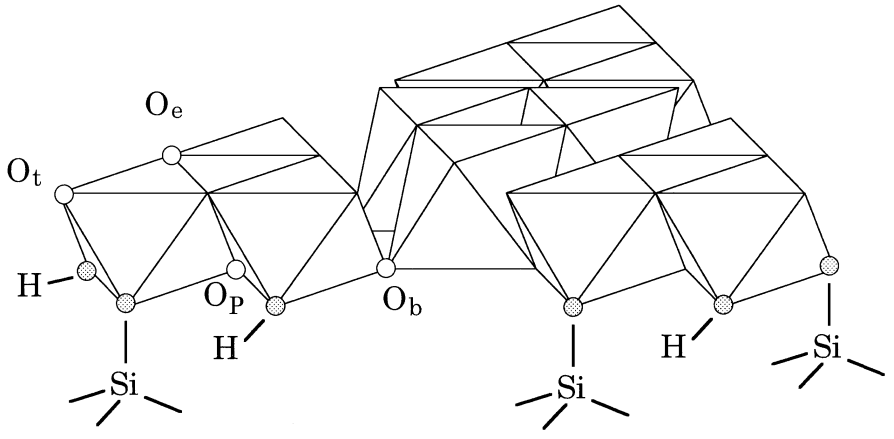

FIG. 13. Model of the planar cluster obtained by transformation of the Keggin unit after opening and grafting onto silica.

The last step (after high temperature calcination) is the molybdenum trioxide crystallization, as unambiguously shown by Raman spectroscopy and XRD. The crystallites formation does not exclude the simultaneous presence on the silica surface of highly dispersed molybdenum oxide species, as proposed by Wachs *et al.* (24, 28) for MoO_x/SiO_2 catalysts submitted to a high temperature calcination.

(2) Decomposition Mechanism of the Keggin Unit

The nature of the intermediate species, obtained after calcination at 400°C is more difficult to determine. On Mg-containing catalysts, the transformation of the Keggin unit affects only the acidity which is almost suppressed by calcination at 400°C, the redox catalytic activity remaining approximately constant. Simultaneously, we do not observe any Raman signal suggesting that the surface species resulting from calcination at 400°C has lost the Keggin structure and does not present a long-range order as in crystallized oxide. The IR spectra show a decrease in the intensity of the 876 cm^{-1} band (ν Mo–O_b–Mo), which could indicate that the bonds connecting two groups of three edge-shared MoO_x octahedra have been broken during calcination at 400°C. Moreover, the disappearance of the 1065 cm^{-1} band (ν P–O in the Keggin unit) confirms the collapse of the Keggin structure. Nevertheless, the presence of all the other IR bands of the Keggin unit could indicate that some parts of the Keggin structure have been preserved. We can then propose that upon calcination at 400°C, the Keggin units are opened by breaking the bridging Mo–O_b–Mo bonds, the resulting species being formed by the three edge-shared MoO_x octahedra group isolated or linked together. The exotherm visible at 390°C could be the result of the grafting of these Mo species onto the silica surface following the two possible reactions:

$$\text{Mo–O–Mo} + \text{Si–O–Si} \rightarrow 2\,\text{Si–O–Mo}$$

or

$$\text{Mo–O–Mo} + \text{Si–OH} \rightarrow \text{Si–O–Mo} + \text{Mo–OH}.$$

The grafting reaction of Mo–OH on Si–OH,

$$\text{Mo–OH} + \text{Si–OH} \rightarrow \text{Mo–O–Si} + H_2O,$$

should not be taken into account since the water formed by this reaction would likely be released in the gas phase and would undergo a decrease of the catalyst weight which has not been observed on the TGA curve at this temperature.

As already proposed (4), the resulting species could be a planar oxide cluster with the same nuclearity as in the Keggin ion (12 Mo atoms). This cluster can be easily formed by breaking half of the Mo–O_b–Mo bonds and by rotating the groups of three edge-shared octahedra around the axis formed by the remaining O_b atoms in order to preserve the Mo–O–Mo angle, as shown in Fig. 13. This planar cluster, grafted onto silica, exposes to the gas phase the same surface structure as in the Keggin ion, but without Brönsted acidity.

(3) Catalytic Behavior

The methanol oxidation being structure sensitive (29–31), the rate and the selectivity are mainly controlled by the surface structure. The constancy of the redox reaction rates after calcination at 400°C are then fully consistent with the preceding model since the structure exposed to the gas phase is not changed. The dimethyl ether formation, which can be considered as a parallel pathway of methanol transformation, is controlled by surface acidity. The disappearance of the Brönsted acidity upon calcination leads to a dramatic decrease in the rate of dimethyl ether formation. The high temperature calcination transforms the bidimensional planar cluster into tridimensional crystallized α-MoO_3 decreasing then the exposed oxide surface, as

revealed by the decrease of the reaction rate (Table 2). For the HPMo/2Mg–SiO_2 sample, the low DME formation rate observed for the fresh sample and its only small decrease after calcination at 400°C could be explained by a higher degree of Mg salt formation on the catalyst surface, due to the excess of Mg cations which are then able to completely neutralize the HPMo species. The 400°C calcination, which suppresses the Brönsted acidity induces then only a small variation in the DME formation rate. The low cristallinity observed by XRD after the 500°C calcination and the constancy of both DME and DHG rates, strongly suggest that an excess of Mg cations (Mg/KU > 1) leads to a better stabilization of the bidimensional planar cluster than a stoichiometric ratio (Mg/KU = 1).

For the HPMo/SiO_2 sample, the situation is quite different, since we have shown by XRD that calcination at 400°C leads to the formation of both α- and β-MoO_3, the β form being the main oxide phase on the silica surface, as observed by Fournier *et al.* (25) on the same system. By high temperature calcination, β-MoO_3 is partly transformed into α-MoO_3, the stable MoO_3 phase at high temperature (16, 17). The catalytic behavior of the fresh catalyst is mainly acidic with a high DME formation rate which can be related to the acidic protons of HPMo species. The higher DHG rates observed on fresh Mg-free samples and the constancy of the DHG rate of HPMo/2Mg–SiO_2 sample whatever the calcination temperature, could be explained by two possible mechanism pathways of redox reactions on HPC species:

—a classical redox mechanism as on crystallized oxide surfaces, implying metal cations and structural oxygen

—a less usual mechanism, as already postulated (27, 32), where the first step is a CH_3OH protonation by acidic protons of HPA species, followed by water elimination leading to the formation of a CH_3^+ species which can be evolved to the DME formation (by further reaction with CH_3OH) and regeneration of the starting proton, or to the formation of a methoxy group by electron transfer from an oxygen belonging to the Keggin unit. After H abstraction by a neighbouring dehydrogenating site, the resulting intermediate species either desorbs to form formaldehyde or further reacts to form methylal and methyl formate.

It was shown (27) that the rate of this reaction pathway depends on the amount of acidic protons able to protonate the CH_3OH molecule. On Mg-containing catalysts, only a small amount of protons are available, due to the salt formation, limiting then the importance of this reaction pathway. On HPMo/2Mg–SiO_2 sample, where we have enough Mg cations to completely form the salt of HPMo, only the clasical redox mechanism can occur, as shown by the constancy of the DHG rate.

The catalytic behavior of HPMo/SiO_2 sample is characterized by a sharp decrease in the overall reaction and dimethyl ether formation rates after calcination at 400°C, due to the disappearance of the Brönsted acidity and the formation of tridimensional crystallized oxide. The maximum observed in the methylal selectivity after calcination at 400°C seems connected to the presence of β-MoO_3 (25). The higher selectivity in dimethyl ether observed on Mg-free sample, even after high temperature calcination could be due to the presence of β-MoO_3 oxide or to the surface phosphorous atoms which induces a Brönsted acidity by phosphoric acid formation, whereas on Mg-containing catalysts, the presence of Mg cations could constitute a basic site neutralizing this acidity.

E. CONCLUSION

The use of different techniques (TGA-DTA, FTIR and Raman spectroscopies, and XRD) and methanol oxidation as a probe reaction has allowed us to follow the thermal transformation of the silica-supported Keggin ion $PMo_{12}O_{40}^{3-}$, in the acid form (HPMo/SiO_2) or in the magnesium salt form (MgPMo/SiO_2 and HPMo/Mg–SiO_2).

The thermal transformation of the $PMo_{12}O_{40}^{3-}$ Keggin unit is deeply modified by the presence of Mg ions on the silica surface which act as a "chemical glue," stabilizing a species intermediate between the Keggin ion and the tridimensional crystallized oxide. This species could be a flat oxide cluster with the same nuclearity and composition as those of the starting Keggin ion, resulting from the opening of the Keggin structure and its grafting onto the silica surface.

Silica surface Mg ions appear to play a double role: first, they create strong interactions between support and HPMo species by surface formation of the partial magnesium salt $Mg_xH_{3-2x}PMo_{12}O_{40}$ ($0 < x < 1.5$) immobilizing then the Keggin units, and second, they stabilize the oxide cluster resulting from the thermal decomposition of the Keggin units. This latter effect is enhanced by increasing the Mg/Keggin unit molar ratio.

Catalytic methanol oxidation has shown that the planar oxide clusters resulting from partial transformation of the Keggin units present a higher selectivity in mild oxidation reaction (DHG and formaldehyde formation) than the undecomposed Keggin units or crystallized molybdenum oxide (α-MoO_3 or β-MoO_3).

In absence of Mg cations, the Keggin unit decomposition occurs approximately at the same temperature (395°C) as observed for the Mg-containing samples, but leads to the direct formation of crystallized molybdenum oxides (α- and β-MoO_3) without formation of the intermediate species.

Experiments are in progress to generalize the results of this work to other alkaline earth cations and different polyanion structures.

REFERENCES

1. Misono, M., *Catal. Rev.-Sci. Eng.* **29**, 269 (1987).
2. Misono, M., *in* "Proc. 10th Int. Cong. Catal., 1992, Budapest, Hungary, New Frontiers in Catalysis," Stud. Surf. Sci. Catal., Vol. 75, p. 69, Elsevier, Amsterdam, 1993.
3. Kozhevnikov, I. V., *Catal. Rev.-Sci. Eng.* **37**, 311 (1995).
4. Brückman, K., Che, M., Haber, J., and Tatibouët, J. M., *Catal. Lett.* **25**, 225 (1994).
5. Malinowski, S., Szczepanska, S., Bielanski, A., and Sloczynski, J., *J. Catal.* **4**, 324 (1965).
6. Gervasini, A., Bellussi, G., Fenyvesi, J., and Auroux, A., *J. Phys. Chem.* **99**, 5117 (1995).
7. Jiratova, K., and Beranek, L., *Appl. Catal.* **2**, 125 (1982).
8. Watanabe, T., Liao, J., and Senna, M., *J. Solid State Chem.* **115**, 390 (1995).
9. Mross, W. D., *Catal. Rev.-Sci. Eng.* **25**, 591 (1983).
10. Niemelä, M. K., Krause, A. O. I., Vaara, T., and Lahtinen, J., *Topics Catal.* **2**, 45 (1995).
11. Tsigdinos, G. A., *in* "Topics Current Chemistry," Springer-Verlag, Berlin, **76**, 1 (1978).
12. Tatibouët, J. M., Montalescot, C., and Brückman, K., *Appl. Catal. A* **138**, L1 (1996).
13. Tatibouët, J. M., *Appl. Catal. A* **148**, 213 (1997).
14. Hodnett, B. K., and Moffat, J. B., *J. Catal* **88**, 253 (1984).
15. Bielanski, A., Malecka, A., and Pozniczek, J., *J. Therm. Anal.* **35**, 1699 (1989).
16. Harb, F., Gérand, B., Nowogrocki, G., and Figlarz, M., *C. R. Acad. Sc. Paris* **303**, 349 (1986).
17. McCarron III, E. M., *J. Chem. Soc., Chem. Comm.*, 336 (1986).
18. Svensson, G., and Kihlborg, L., *React. Solids* **3**, 33 (1987).
19. JCPDS Files, 35-609 (α-MoO_3); 37-1445 (β-MoO_3).
20. Parise, J. B., McCarron III, E. M., Von Dreele, R., and Goldstone, J. A., *J. Solid State Chem.* **93**, 193 (1991).
21. Parise, J. B., McCarron III, E. M., and Sleight, A. W., *Mat. Res. Bull.* **22**, 803 (1987).
22. Rocchiccioli-Deltcheff, C., Amirouche, M., Hervé, G., Fournier, M., Che, M., and Tatibouët, J. M., *J. Catal.* **126**, 591 (1990).
23. Rocchiccioli-Deltcheff, C., Fournier, M., Franck, R., and Thouvenot, R., *Inorg. Chem.* **22**, 207 (1983).
24. Banares, M. A., Hu, H., and Wachs, I. E., *J. Catal.* **155**, 249 (1995).
25. Fournier, M., Aouissi, A., and Rocchiccioli-Deltcheff, C., *J. Chem. Soc., Chem. Comm.*, 307 (1994).
26. Tatibouët, J. M., Che, M., Amirouche, M., Fournier, M., and Rocchiccioli-Deltcheff, C., *J. Chem. Soc., Chem. Comm.*, 1260 (1988).
27. Brückman, K., Tatibouët, J. M., Che, M., Serwicka, E., and Haber, J., *J. Catal.* **139**, 455 (1993).
28. Banares, M. A., Hu, H., and Wachs, I. E., *J. Catal.* **150**, 407 (1994).
29. Tatibouët, J. M., and Germain, J. E., *J. Catal.* **72**, 375 (1981).
30. Tatibouët, J. M., and Germain, J. E., *C. R. Acad. Sci. Paris* **296** II, 613 (1983).
31. Ziolkowski, J., *J. Catal.* **100**, 45 (1986).
32. Highfield, J. G., and Moffat, J. B., *J. Catal.* **95**, 108 (1985).